EngOpt 2008 - International Conference on Engineering Optimization
Rio de Janeiro, Brazil, 01 - 05 June 2008.

Multi-Objective Optimization of Free-Form Grid Structures

P. Winslow[1], S. Pellegrino[2], S.B. Sharma[3]

[1] Cambridge University, Engineering Department, Trumpington Street, Cambridge CB2 1PZ, UK
(pjw63@cam.ac.uk)
[2] California Institute of Technology, Pasadena, California 91125, USA
[3] Buro Happold Ltd, Camden Mill, Lower Bristol Road, Bath, BA2 3DQ, UK

1. Abstract
Computational modeling software facilitates the creation of any surface geometry imaginable, but it is not always obvious how to create an efficient grid shell structure on a complex surface. This paper presents a design tool for synthesis of optimal grid structures, using a Multi-Objective Genetic Algorithm to vary rod directions over the surface in response to two or more load cases. A process of grid homogenization allows the tool to be rapidly applied to any grid structure consisting of a repeating unit cell, including quadrilateral, triangular and double layer grids. Two case studies are presented to illustrate the successful execution of the optimization procedure.

2. Keywords: Structural optimization, multiobjective, grid shell.

3. Introduction
The advent of free-form 3-D modeling software has allowed architects and designers to create any shape imaginable. In order to physically realize these computer models, say as a building or a sculpture, an internal armature can be used along with non-load bearing panels to create the required external surface e.g. Gehry's Guggenheim Museum in Bilbao. Use of a 'grid-shell' structure, consisting of a lattice of rods (see Figure 1) may be more desirable due to the potential for reductions in material usage and increased internal space. However, it is not always obvious how to create an efficient grid structure on a given surface.

The need for new computational structural engineering tools that can be applied to complex geometries has been highlighted by several authors, including Schlaich at al. [1]. Michalatos et al. [2] describe a number of new tools for grid mapping. In general, the task of creating an efficient grid structure is made more difficult by the diverse range of requirements on architectural engineering projects, which might include: ultimate limit failure criteria, serviceability/comfort criteria for a variety of load cases, and aesthetics. As such, a conventional optimization algorithm which finds a single 'best' structure may not be desirable since it can restrict overall design freedom. Therefore this paper will present a novel method for synthesis of grid structures on free-form surfaces, which utilizes a Multi-Objective Genetic Algorithm (MOGA) to find optimal rod orientations.

Figure 1: British Museum Great Court Roof, London, UK (Courtesy of Andrew Dunn)

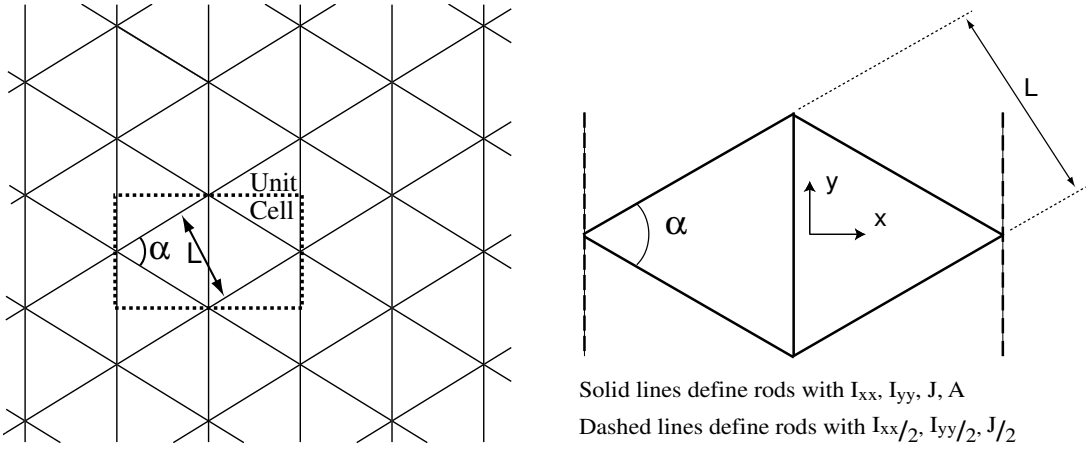

(a) Regular triangulated grid

(b) Unit cell

Figure 2: Definition of repeating unit cell for a triangulated grid of rods

Topology optimization can be used to create an efficient structure on a given surface, as described by Maute and Ramm [3]. However, the solutions obtained are akin to a continuum shell with holes cut away, and so complex post-optimization rationalization would be required to convert this into a structure consisting of discrete rods and nodes. To avoid this requirement, the algorithms developed in this paper are based on techniques for finding optimal orientation of fibres in a composite, e.g. [4]. Although the final structure must be a set of discrete rods, a process of homogenization allows for the lattice of rods to be represented by anisotropic continuum shell finite elements throughout the optimization process. A novel parametrization of the problem reduces the number of design variables, thus making the use of a MOGA more feasible and improving the constructibility and visual appeal of optimized designs. The basis of this approach was first described by the authors [5], but this current paper describes significant new developments to the method and explores the use of a MOGA in detail.

4. Homogenization

The algorithm described in this paper is based upon the lattice of rods being represented by an anisotropic continuum material of equivalent stiffness. The optimization can therefore be applied to any structure consisting of a repeating unit cell, such as a triangulated single layer grid (see Figures 1 and 2(a)), a quadrilateral single layer grid or a double layer space frame. A novel aspect of the approach used in this paper is that we consider a variable geometry for the unit cell. So for the triangulated unit cell shown in Figure 2(b) the angle α is a variable. The anisotropic continuum material stiffness matrix (Eq. 1), which is a function of α, is derived from the the unit cell and relates extensional strains and curvatures to membrane forces and bending moments. Periodic boundary conditions are used to calculate this matrix for any given unit cell geometry, as described by [7]. Full details of how this technique is implemented for a variable geometry unit cell are given in [5].

$$\begin{bmatrix} N_x \\ N_y \\ N_{xy} \\ M_x \\ M_y \\ M_{xy} \end{bmatrix} = \begin{bmatrix} A_{11} & A_{12} & A_{16} & B_{11} & B_{12} & B_{16} \\ A_{21} & A_{22} & A_{26} & B_{21} & B_{22} & B_{26} \\ A_{61} & A_{62} & A_{66} & B_{61} & B_{62} & B_{66} \\ B_{11} & B_{12} & B_{16} & D_{11} & D_{12} & D_{16} \\ B_{21} & B_{22} & B_{26} & D_{21} & D_{22} & D_{26} \\ B_{61} & B_{62} & B_{66} & D_{61} & D_{62} & D_{66} \end{bmatrix} \begin{bmatrix} \varepsilon_x^0 \\ \varepsilon_y^0 \\ \varepsilon_{xy}^0 \\ \kappa_x \\ \kappa_y \\ \kappa_{xy} \end{bmatrix} \tag{1}$$

5. Solution Representation

In order to optimize the homogenized structure one could assign two independent design variables to every shell element in the FE mesh (angle between the rods α, and rotation of the principal material

directions β). However, from a practical point of view this is unnecessary; we hope to obtain structures with some degree of rod continuity and with limited curvature, so that it is both constructible and visually appealing. Therefore the 'designer' chooses a number of points on the surface Ω at which α and β are independently defined, see Figure 3. Piece-wise linear interpolations are then used to define α and β at the centroid of every finite element between these 'design points'. So, for instance, if the surface Ω was meshed with shell elements, any element centroid lying within the gray shaded region would be assigned rod angles based on a linear interpolation of α_2,α_4,α_7 and β_2,β_4,β_7 . The interpolation patches can be created manually or by Delaunay triangulation of the 'design' points in the surface parameter domain. Note that quadratic interpolation patches could be used if mid-side design points were defined; it is simply a sub-class of the same problem.

Given that the surface Ω may by highly curved, it is necessary that the rod angles are defined relative to local coordinate systems (the direction of which must vary smoothly over the surface). In this paper all surfaces are represented using NURBS, thus they have an underlying (u, v) parametrization. At any point on the surface we can therefore define rod angles to be measured clockwise from the positive u-direction, as shown in Figure 4. For surfaces with complex topology each region becomes a chart with its own (u, v) parametrization, and transition functions ensure continuity between charts (as is well established in field of discrete differential geometry [6]).

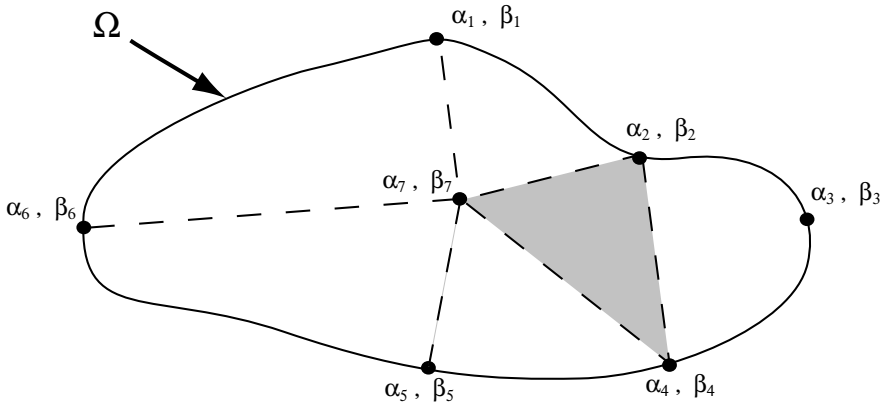

Figure 3: Subdivision of surface Ω into regions using 7 points

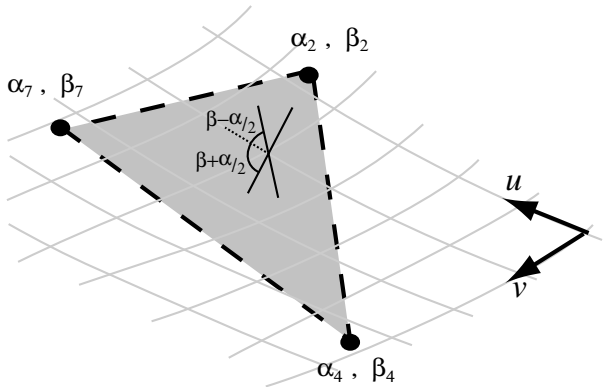

Figure 4: Single region (from Figure 3), shown with underlying (u,v) surface parametrization. Angles of the two sets of rods, $\beta + \alpha/2$ and $\beta - \alpha/2$, are measured anti-clockwise from local u-axis (dotted line)

The above procedure ensures that there is tangent continuity of the rods between the interpolation patch region. However, it relies upon having a surface parametrization with low distortion of angles

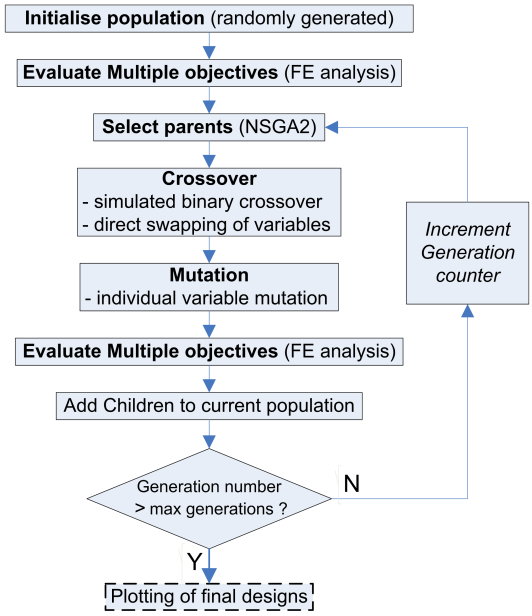

Figure 5: Multi-objective optimization procedure

and lengths. For many surface geometries it is possible to obtain a satisfactory surface parameterization from commercially available CAD packages. Creation of low distortion surface parameterizations for any given surface has been addressed in the field of computer graphics [6].

Although commonly used in genetic algorithms, a bit string solution encoding is not used here for a number of reasons:

- Use of real numbers allows continuous variables to be represented exactly.
- Simulated binary crossover [8] allows real-numbered representations to be successfully evolved.
- A one dimensional bit string would result in loss of the surface geometry and regional connectivity information when considering crossover and mutation operators.

The data used to represent each solution is therefore:

1. Real numbered values of α_i and $\beta_i$for all region corner nodes
2. Connectivity of each region (i.e three corner node numbers) for use by cross-over operators.

6. Optimization Scheme

The flow chart in Figure 5 shows the multi-objective optimization procedure. The aim is to minimize a number of objectives

$$f_1(\boldsymbol{\alpha}, \boldsymbol{\beta}), f_2(\boldsymbol{\alpha}, \boldsymbol{\beta}).....f_n(\boldsymbol{\alpha}, \boldsymbol{\beta}) \tag{2}$$

subject to

$$(0 + \sigma) < \alpha_i < (180 - \sigma) \tag{3}$$

$$0 < \beta_i < 180 \tag{4}$$

where:

σ=minimum allowable angle between the rods

i=design point number

The flowchart is explained in more detail by the sub-sections below.

6.1. Selection
A key part of the optimization process is selection of suitable parents from which the next generation of designs will be evolved. For this purpose an elitist algorithm, the Non-dominated Sorting Genetic Algorithm II (NSGA-II) [9], is used since it has been shown that for most multi-objective test problems elitist algorithms perform better than other selection methods. NSGA-II chooses parents using not only their fitness but also by considering their spread. Thus a more diverse Pareto-optimal front is generated and so there is greater freedom when choosing a design from the final population. The PISA implementation of NSGA-II [10] is used for this paper.

6.2. Crossover Operators
For this paper two specific operations are used to create new designs from a pair of parents:

1. Simulated binary crossover (SBX)

   A real-valued representation of designs is used, so standard bit string one point cross-over operators are not applicable. However, simulated binary cross-over [8] overcomes this limitation whilst allows retention of the other benefits associated with a real valued representation.

2. Uniform crossover

   Direct swapping of a design variable between two parents (c.f. two-point bit-string crossover)

6.3. Mutation Operators
A mutation operator is used which considers each real-numbered design variable in turn. A random number is generated and if it is less than the pre-specified mutation probability then that design variable is mutated. A non-uniform probability density function is used so that small changes in the design variable have a high likelihood of occurrence, whilst larger mutations are rare.

7. Rod Plotting
Plotting of rod paths to give a complete grid structure is a post processing step, outside the main optimization loop. For a given design α and β are defined everywhere on the surface (see Section 5.). The local coordinate systems (from which these angles are measured) are known, hence it is a trivial matter to create a pair of vector fields on the surface which define the directions of the two primary sets of rods. Note that these directions are defined by angles $\beta + \alpha/2$ and $\beta - \alpha/2$, see Figure 4. Drawing the rod paths is then a case of finding sets of lines which are tangential to these vector fields.

A simple step-wise plotting algorithm is used for this paper. The user picks a start point (which may be the top of a column, apex of a dome etc.), and a path is drawn from that point in a step-wise manner such that it is tangential to one of the vector fields everywhere along its length (c.f. plotting of a streamline in fluid flow). This process is repeated until the desired density of rods is achieved. For a triangulated grid, the two primary directions are drawn first and triangulation is added afterwards. Research into an automated rod plotting algorithm (such as the techniques described by Michalatos et al. [2] and Tong et al. [6]) is currently underway and details will be published elsewhere.

8. Example I
The first illustrative example is a dome subject to two eccentric load cases. The surface is a spherical cap with a height of 25 m, cut from a sphere of radius 174.5 m (cap diameter is 180 m), see Figure 6(a). Also shown in this figure are three support points which are fixed against translation, and the surface is shaded according to the wind load objective (see below). The objectives are:

1. Minimize deflection under combined self-weight and asymmetric wind loading. Referring to Figure 6(a) the dark grey area (upwind 1/3 of the surface) is subject to +2 kPa, light gray area (downwind 2/3 of surface) is subject to -1 kPa).

2. Minimize deflection under combined self-weight and 2 m/s^2 lateral acceleration (indicative of the peak acceleration in an earthquake)

The structure is to be constructed from a triangulated grid of rods (see Figure 6(b)) with perpendicular spacing L = 5 m. However, given the large span of this dome each 'rod' is a 5 m deep planar truss

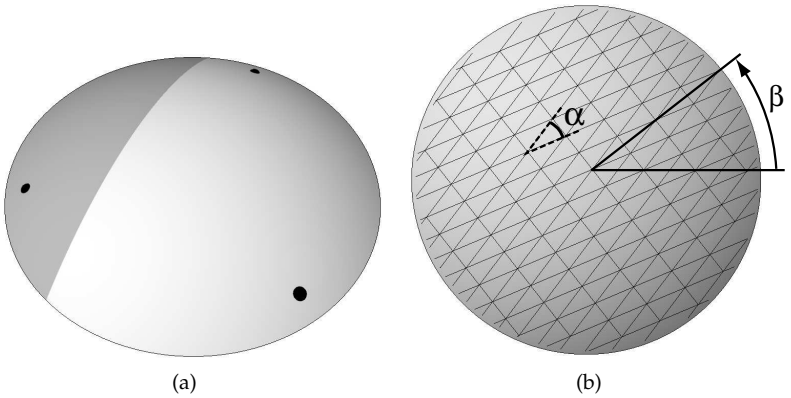

Figure 6: Spherical cap problem definition. (a) Support points shown in black, and wind loading zones by gray shading. (b) Schematic definition of rod angles

made from 0.5 m diameter steel tubes of wall thickness 0.05 m. It is straightforward to implement this more complex structure because the homogenized stiffness matrix is simply calculated using values of I_{xx}, I_{yy}, J, A which are representative of a truss rather than of a single tube.

For simplicity in this preliminary example each grid design is represented by two design variables

$$10 < \alpha < 170 \quad \text{and} \quad 0 < \beta < 180$$

as shown in Figure 6(b). Thus design space is represented by a pair of contour plots:

Wind loading objective = F(α, β) in Figure 7 and *Earthquake objective* = F(α,β) in Figure 8.

These contour plots are created numerically by evaluating the objective functions for many different values of α and β. This allows us to readily visualize the progress of the genetic algorithm. Starting with an initial population of 20 random designs, the evolving population is plotted at generation numbers 1,5 and 20 on a trade-off plot (Figure 9) and on the two contour plots (Figures 7 and 8). Note that the scale on Figure 9 is enlarged, thus many designs in generation 1 are not visible.

Also included on the trade-off plot (Figure 9) is the optimal Pareto-front. This has been calculated numerically from the two contour plots, and gives a effective visual indication of how rapidly the genetic algorithm is converging towards the optimum. A commonly used measure of convergence is the mean Euclidean distance between all designs in a given generation and the optimal Pareto-front [8]. For this example the convergence is very rapid; after just 20 generations the mean Euclidean distance is 1.7×10^{-4} (which is $\approx 0.1\%$ of the value of the objective functions).

It is interesting to note that in Figure 7 a number of the designs in the 20th generation have converged to a minima where the value of β is very near its upper limit of 180 degrees. The maximum value of β in the initial population is $\approx$ 160, so this evolution between the 1st and 20th generations would not be possible by cross-over alone. Hence it appears that the mutation operator is crucial in problems where there is a minima near the limits of design variables. A study was carried out to investigate the effect of the genetic algorithm parameters on the rate of convergence. Using the mean and standard deviation of the Euclidean distance (as described above), the following probabilities were found to give good convergence: SBX = 0.6, Variable swap = 0.2 and Non-uniform mutation = 0.2.

9. Example II

For the second example a 54 m span doubly-curved arch will be considered. The surface, shown in Figure 10(a), is fixed against translation at both ends. The grid structure will be constructed from a bi-directional grid of steel tubes with aluminium infill panels. The steel tubes are 114.3 mm in diameter and have 5 mm wall thickness. The panels are 2 mm thick, and it is assumed that they are rigidly attached to the bi-directional grid. The perpendicular spacing between the rods is taken as 0.5 m,

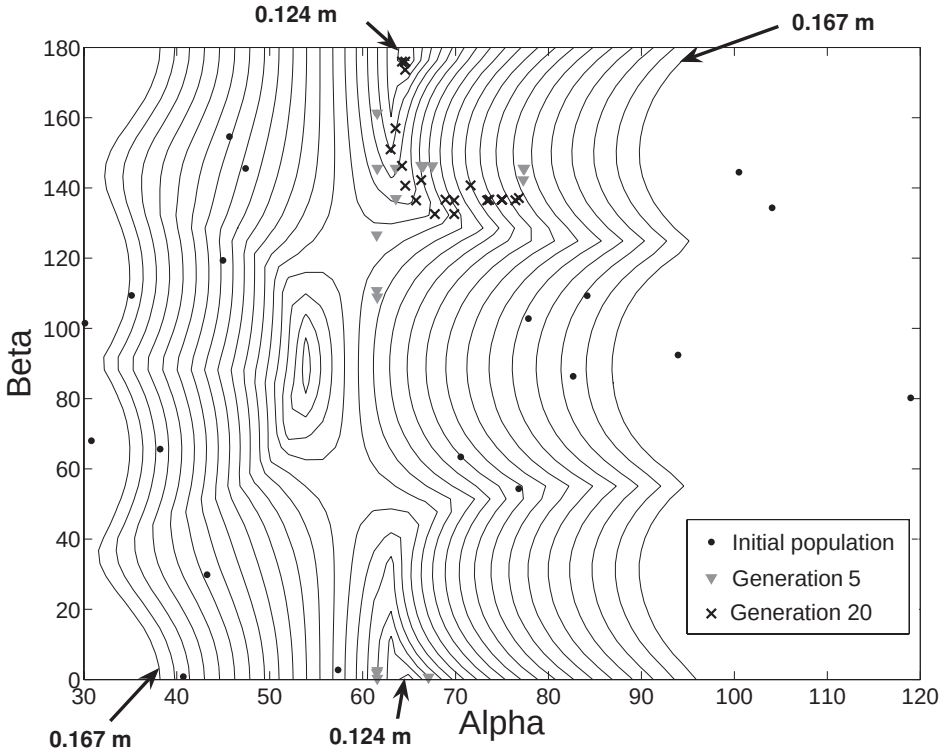

Figure 7: Contour plot of objective 1 (deflection due to wind) with genetic algorithm results

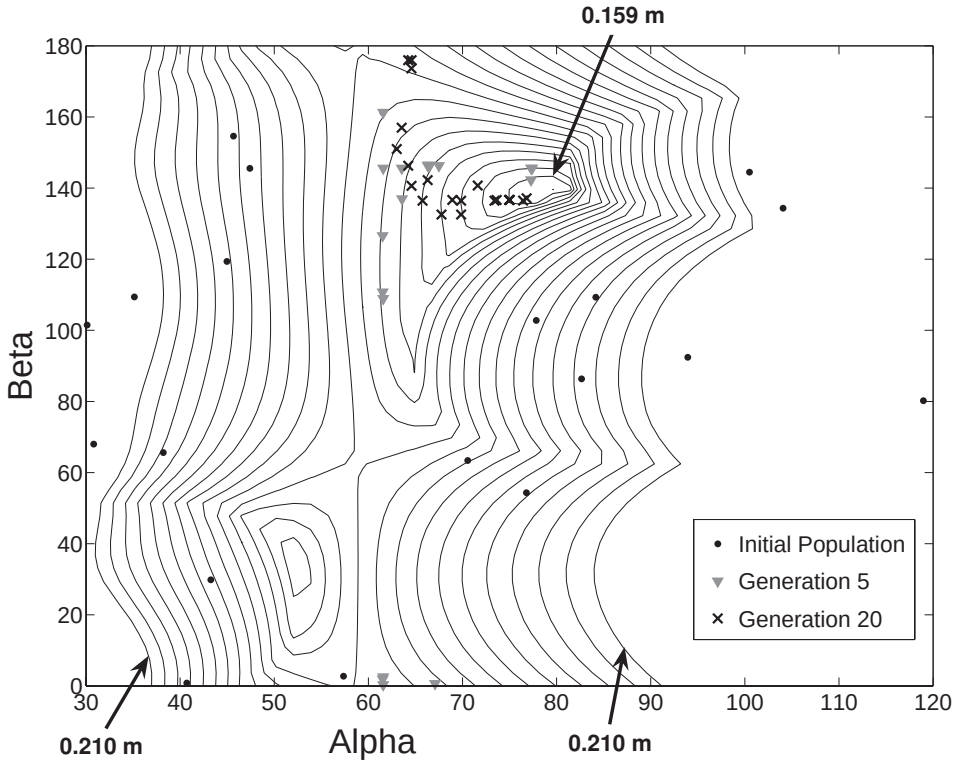

Figure 8: Contour plot of objective 2 (earthquake deflection) with genetic algorithm results

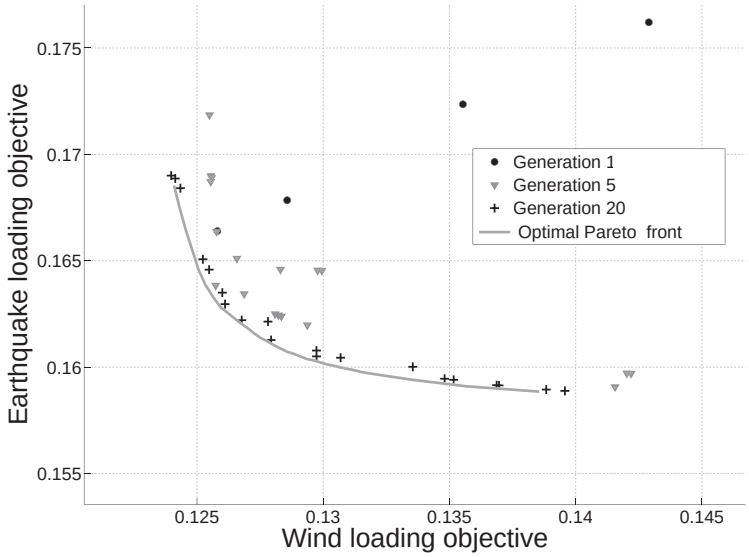

Figure 9: Trade-off plot for generations 1, 5, 20, and optimal Pareto-front

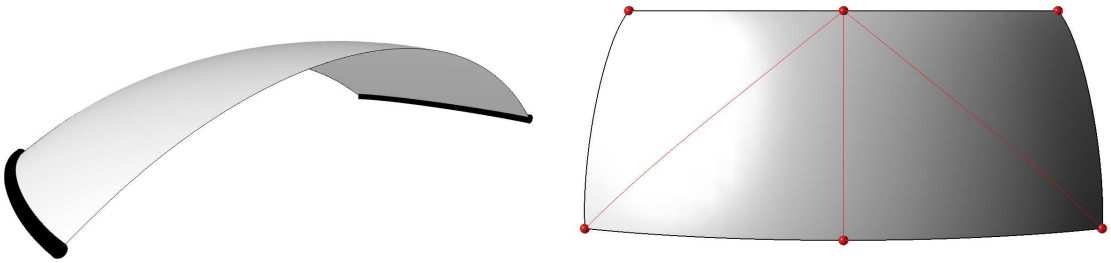

(a) (b)

Figure 10: Example II problem definition. (a) Doubly curved surface geometry, with end supports shown in black (b) Surface subdivision scheme (6 design points, 4 regions)

which means that the total length of rods in the structure is fixed. Therefore total structural mass is constant throughout the optimization. Two objective functions are considered:

1. Minimize deflection under combined self-weight and asymmetrical wind loading from the prevailing direction (see Figure 11(a))

2. Minimize deflection under combined self-weight and symmetrical wind loading from direction 2 (see Figure 11(b))

The surface is divided into a number of regions; 6 design points are chosen for this example, giving 4 regions and 12 design variables (see Figure 10(b)). A population size of 100 is used, and the initial population is generated randomly.

The results from 50 generations of evolution are shown in Figure 12. It should be noted that only some of the designs from the initial population can be seen on this chart, since the others are off the scale. By the 50th generation a very clear trade-off surface of optimal designs has evolved, and two of these are plotted in Figures 13(a) and 13(b). A rendered image of Design 2 is shown in Figure 14. Visual inspection of these diagrams shows that the latter design (which is optimal for the symmetric wind load case) is very close to being symmetrical; the mean difference between rod angles at one region corner node and the opposing corner node is $\sim$5 degrees. Hence despite not enforcing symmetry (e.g. by only

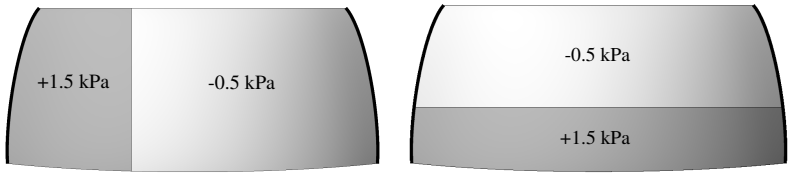

(a) Asymmetrical wind loading (b) Symmetrical wind loading

Figure 11: Wind loading definition for example problem II

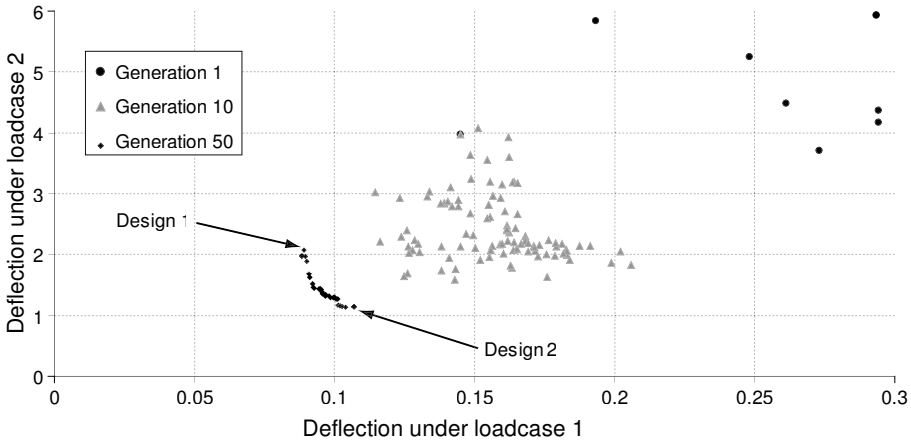

Figure 12: Trade-off plot showing design evolution over 50 generations

considering half of the structure) the genetic algorithm has converged to a logical, rational solution. The small amount asymmetry in Figure 13(b) could be reduced further by adopting a self-adaption approach (more akin to Evolution Strategies) whereby the probability and magnitude of any mutations is reduced in later generations, hence increasing the ability to converge to the optimum.

9. Conclusions and Further Work

A novel tool for multi-objective optimization of grid structures has been presented in this paper. Given a surface and a desired grid type it has been shown, by example, that the rod orientations can be successfully evolved to create a population of optimal designs. The homogenization process allows us to synthesize any type of grid structure provided it has a repeating unit cell e.g triangular, double-layer or quadrilateral with infill panels etc.. The sample problems presented in this paper suggest that using

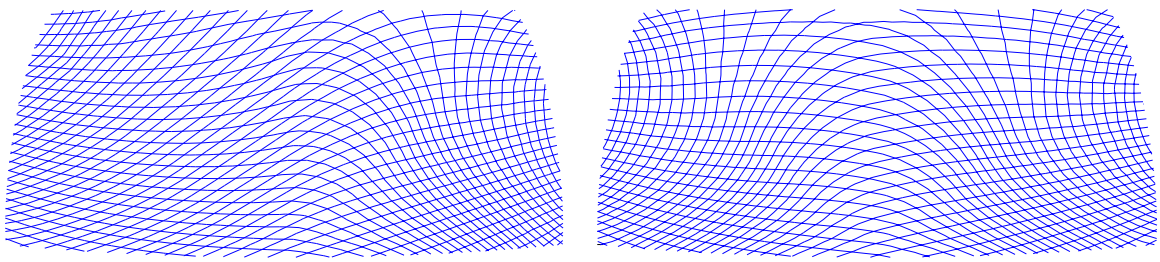

(a) Design 1: High stiffness for load case 1 (b) Design 2: High stiffness for load case 2

Figure 13: Two designs from 50th generation.

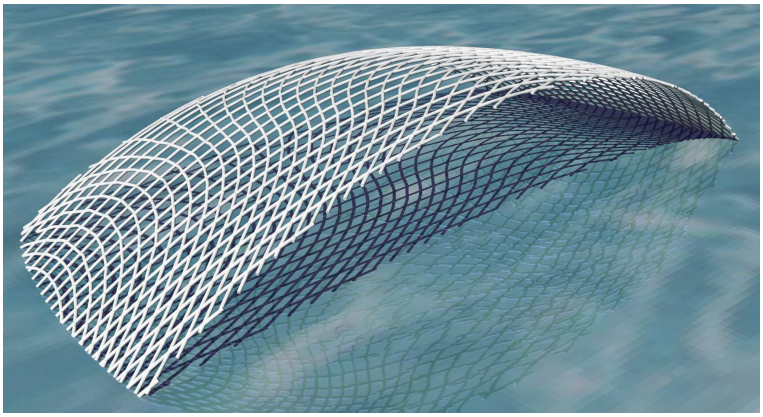

Figure 14: Design 2

a relatively modest number of generations it is possible to evolve a diverse range of solutions, which appear constructible and visually rational.

The main direction of future research is to develop a reliable automated scheme for plotting optimized rod paths. It is envisaged that this will form part of a second-pass optimization and refinement tool, in which the objective functions are evaluated by FE analysis of the discrete grid of beams/rods.

10. Acknowledgements

We would like to acknowledge the financial support of the UK Engineering and Physical Sciences Research Council and of Buro Happold.

12. References

[1] Schlaich, J., Schober, H. and Kurschner, K., New Trade Fair in Milan - Grid Topology and Structural Behaviour of a Free-Formed Glass-Covered Surface, *International Journal of Space Structures*, 2005, Vol 20, pp1-14.

[2] Michalatos, P. and Kaijima, S., Design in a non homogeneous and anisotropic space, *International Association of Shell and Spatial Structures Symposium 2007, Venice, Italy, December 3-6*, 2007.

[3] Maute, M. and Ramm, E., Adaptive topology Optimization of Shell Structures, *AIAA journal*, 1997, Vol 35, No. 11, pp1767-1773

[4] Gurdal, Z., Olmedo, R., In-plane response of laminates with spatially varying fiber orientations. Variable stiffness concept, *AIAA Journal* , 1993, Vol. 31, pp751 - 758

[5] Winslow, P., Pellegrino S. and Sharma S.B., Mapping two-way grids onto free-form surfaces, *International Association of Shell and Spatial Structures Symposium 2007, Venice, Italy, December 3-6*, 2007.

[6] Tong, Y., Alliez,P., Cohen-Steiner, D. and Desbrun M., Designing quadrangulations with discrete harmonic forms, *SGP '06: Proceedings of the fourth Eurographics symposium on Geometry processing, Cagliari, Italy*, 2006,pp201-210

[7] Kueh, A.B.H. and Pellegrino, S., ABD matrix of single-ply triaxial weave fabric composites, *48th AIAA/ASME/ASCE/AHS/ASC Structures, Structural Dynamics, and Materials Conference*, 2007.

[8] Deb, K., Multi-Objective Optimization using Evolutionary Algorithms, *Wiley* 2001.

[9] Deb, K., et al., A fast elitist non-dominated sorting objective genetic algorithm for multi-objective optimization: NSGA-II, *Proceedings of the Parallel Problem Solving from Nature VI (PPSN-VI)*, 2000

[10] Bleuler, S. et al., PISA – A Platform and Programming Language Independent Interface for Search Algorithms, *Conference on Evolutionary Multi-Criterion Optimization*, 2003